PROCEEDINGS OF SCIENCE

Studies of CosmicWatch spectra for students' use

Takeshi Nakamori,[a,*] **Haruki Iiyama,**[a] **Manami Sawai,**[b] **Yuto Hoshi,**[c] **Atsushi Kadota,**[d] **Yuito Oyamada,**[d] **Nana Kobayashi,**[e,f] **Chizuru Nose,**[f,g] **Kyoka Maruta**[f,g] **and Kazuo S. Tanaka**[f,h]

[a] *Yamagata University,*
1-4-12 Kojirakawa, Yamagata, Japan
[b] *Kawawa Senior High School,*
2226-1 Kawawa, Tsuzuki, Yokohama, Japan
[c] *Musashi Junior High School,*
1-26-1 Tokyotamakami, Nerima, Tokyo, Japan
[d] *Sendai Daisan High School,*
1-19 Tsurugaya, Sendai, Japan
[e] *Tokyo Denki University,*
5 Senju-Asahicho, Adachi, Tokyo, Japan
[f] *Accel Kitchen,*
6-3 Aoba, Aramaki, Aoba, Sendai, Japan
[g] *Tohoku University,*
6-3, Aoba, Aramaki, Aoba, Sendai, Japan
[h] *Waseda University,*
3-4-1 Ohkubo, Shinjuku, Tokyo, Japan

E-mail: nakamori@sci.kj.yamagata-u.ac.jp

Many junior and high school students are interested in studying particle physics or astro(particle) physics through their researches, sometimes within school activities and sometimes not. Measuring cosmic rays are one of the easy ways to provide such opportunities without any accelerators or beam facilities. However, in most schools or teachers, preparing and handling detectors may be significant obstacles. CosmicWatch is a USB bus-powered cosmic ray muon detector with a plastic scintillator and a SiPM, which we have adopted and distributed among Japanese school students for their activities. CosmicWatch records the ADC values corresponding to the pulse height of triggered events, and its spectra are very useful in extracting qualified cosmic muon events. In order to do so we need to well understand the spectral feature or components in advance and such studies can also be students' researches. In this paper, we report several studies focusing on the spectra obtained by CosmicWatches – for example, the response dependencies on the interacting position of the scintillator, or induced particle types. These findings will be useful for many students in the future.

38th International Cosmic Ray Conference (ICRC2023)
26 July - 3 August, 2023
Nagoya, Japan

*Speaker

PoS(ICRC2023)1603

1. Introduction

As in other countries and regions, there is a growing societal need for STEM, STEAM, etc. education in Japan. While topics related to astroparticle physics are popular with students as inquiry-based learning subjects, there are difficulties in implementation in general schools. This situation may be due to problems with teaching resources or a lack of experimental equipment. In this context, the Accel Kitchen LCC was launched after forming a framework called Tan-Q[1, 2], in which researchers and mentor university students support, mainly online, junior and high school students in their research activities[3, 4].

CosmicWatch (CW) is a small and inexpensive desktop cosmic ray muon detector developed by Axani et al. [5]. Since this device is very convenient for students and can be mass-produced inexpensively, Accel Kitchen has widely applied, including production, distribution, and support for data analysis. The original design of CW consists of a plastic scintillator of $\sim 5 \times 5 \times 1\,\mathrm{cm}^3$, and a silicon photomultiplier (SiPM) supplied by SensL Technologies, Ltd. Arduino Nano is implemented and responsible for the data acquisition, which is triggered when the pulse height exceeds a threshold value. The recorded data for each trigger consists of the analog-to-digital converter (ADC) value of the pulse height, time stamp, and environmental data such as temperature and air pressure. Its printed circuit board (PCB) pattern and Arduino image files are available as open source.

In this paper, we report the current status of several studies focusing on the ADC spectra obtained by CWs with and without advanced customization. Most of the following work are conducted by students in the authors supported by Accel Kitchen LLC.

2. Case 1: Spectral analysis

2.1 Sub-components and temperature dependency

In the previous study [2], students used CWs and examined the differences in the muon count rate for the height and locations of the observations. They selected good quality muon events acquired by CWs, cut by the ADC value, and calculated the count rate. The resulting count rate was strongly dependent on the cut threshold, a problem when comparing multi-site observations. In addition, there may be individual variations in the ADC spectra among CWs, due to, for example, subtle differences in assembly, the gain of the SiPMs, and the noise level of the circuit. To reduce the ambiguity of such features and to find an ideal threshold, we analyzed the data set measured by a single CW over an extended period of time; the data archived at Accel Kitchen and collected during the student research [7]. This data was collected continuously indoors at Akita High School for over a year.

The monthly ADC spectra appear to have an annual variation, probably due to a temperature cycle throughout the year. The upper left panel of Figure 1 shows examples of the spectra for January and July 2021. As can be seen in the figure, there appear to be several components and the spectral shape varies continuously throughout the year. Fitting by five Gaussians, G1–5, reproduces the spectra well, as shown in the upper right panel of Figure 1. However, we still do not find the counterparts of each Gaussian component. In general, the Gaussian response means that the energy deposition is expected to be nearly monochromatic.

We generated ADC spectra for each temperature measured by CW for the entire year of data. Since the exposure time is different for each temperature, we normalized the data for each temperature bin (5°C in this case), and the relative rate distribution is shown in the bottom panel of Figure 1. Since the SiPM gain increases with lower temperatures, an effect of increasing pulse height can be seen for ADC values above ~ 200 indicated by the solid arrows. These components should correspond to G1, G3 and G4, suggesting that they are due to scintillation events with particles. It can also be seen that the component below 200, namely G5 indicated by the dashed arrow, shifts to the left as the dark count decreases. Interestingly, G4 indicated by the dot-dashed arrow appears to be fixed around 600 regardless of the temperature.

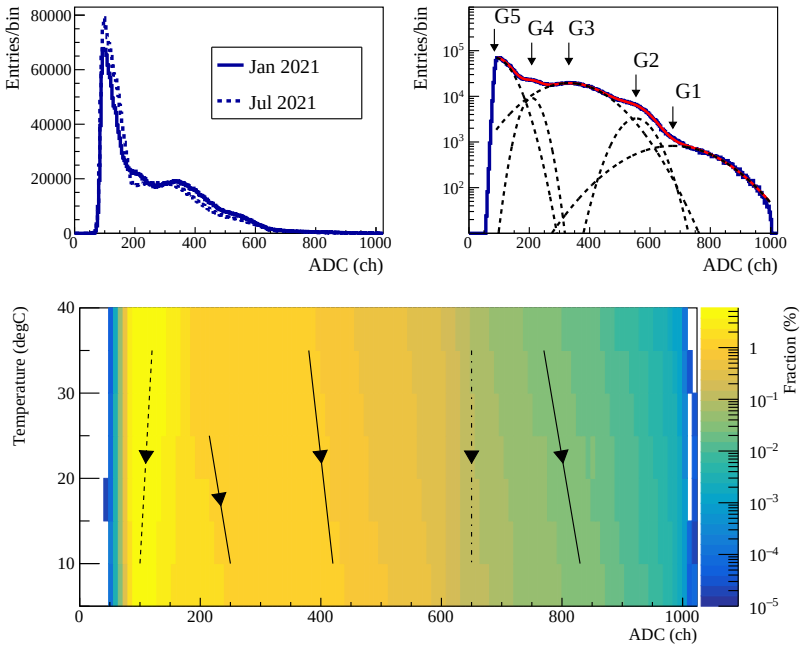

Figure 1: (Upper left) Examples of ADC spectra. Those acquired in January and July 2021 are represented by solid and dashed lines, respectively. (Upper right) The result of the multi-Gaussian fit to the January 2021 data. Arrows with reference names, G1–5, indicate the mean of the corresponding Gaussian. (Bottom) The temperature dependence of the ADC spectra obtained from the 1 year data set. The arrows are a rough guide to the trend of the G1–5 components, see text for details.

2.2 Position dependency

Since the plastic scintillator of the CW is flat and the SiPM of the readout is mounted in the center of the square surface, the collection efficiency of the scintillation light as a function of the incident position should be considered. In order to evaluate the focusing efficiency depending on the incident position of the particles, ^{90}Sr β rays were collimated and irradiated onto a CW scintillator, and the resulting spectra were compared. The CW used in this study is different from that used in the previous subsection.

The spectra obtained by irradiating the scintillator at the center, edge, and corner are shown in Figure 2 (left). Each data set includes muons and background, which is estimated to be about 20%

of these data from another measurement without the β source. Although the β-ray energy spectrum is continuum, by comparing the histograms of each, changes in the light collection efficiency can be extracted. Figure 2 (center) and (right) show the difference between the center and the edge, and the difference between the center and the corner, respectively. It can be seen that there is an excess at the lower ADC value and that the light intensity decreases away from the center where the SiPM is placed. In the case of the SiPM placed in the corner, a chi-squared fit using light intensity as a parameter for collection efficiency shows a decrease of approximately 18%. The scintillator used in this study is wrapped in a multilayer film called ESR, which has a high reflectivity. On the other hand, the one used in the previous chapter is wrapped in aluminum foil, which is expected to have higher transport losses than ESR. Even with this estimate, the origin of each of the five Gaussian components is still uncertain.

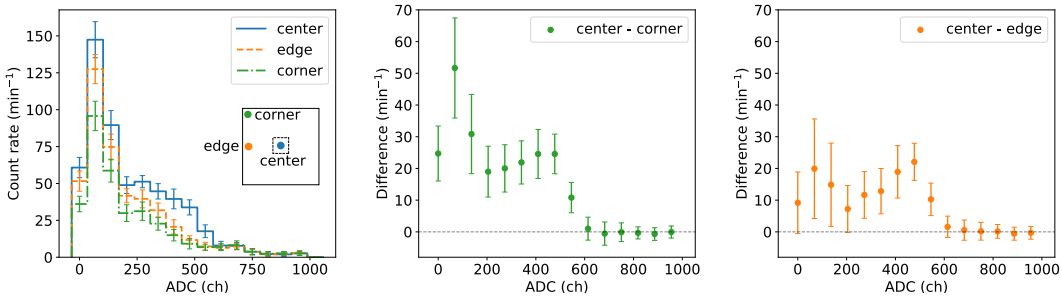

Figure 2: (Left) ADC spectra with collimated β irradiation at different positions. The positions 'center' (solid), 'edge' (dashed) and 'corner' (dot-dashed) are also shown with the scintillator (outer solid square) and the SiPM (inner dashed). The solid, dashed, and dot-dashed lines correspond to the data with the center, edge, and corner irradiation data, respectively. (Middle) and (right) are the difference of the histogram for center vs. edge and center vs. corner, respectively.

3. Case 2: Particle identification with a cloud chamber

We took a different approach to studying CW spectra and their correspondence to different particles. In this study, students from Kawawa Senior High School and Musashi Junior High School developed a hybrid radiation detector that combines a CW and a cloud chamber, in which we can observe particle tracks.

First, we set up a small cloud chamber cooled by a Peltier device[8] and captured particle tracks as a video with a smartphone camera. Then we performed a stand-alone acquisition test and identified incident particles in the movie by eye. Figure 3 (a-c) shows examples of the recorded tracks. We can distinguish linear tracks of muons, tracks of multiple scattering electrons, and α rays with large energy deposits.

After confirming the operation of the cloud chamber, we set up the chamber system with a CW, as shown in Figure 3(d). With this setup, we aimed by this arrangement that particles penetrating the fiducial volume of the chamber would also hit the plastic scintillator of the CW. We performed CW data acquisition on a laptop PC and simultaneously displayed the camera image on the same PC. We then made a video recording of the PC screen for 244 minutes. The CW data acquisition

software outputs the acquired data to the terminal on each trigger so that the track image can be retrieved later when the CW detects the particle.

We played back the recorded video at $0.1-0.5\times$ speed, performed the visual track classification, and recorded the corresponding ADC values. Figure 4 shows the ADC spectra of the acquired CW, superimposed with the distribution of all triggered events, events tagged from the movie as β-like and μ-like. The spectrum of β-like events seems to be similar to the total event distribution, while the μ-like events do not exist below an ADC of 200. Although a firm conclusion cannot be drawn due to the small number of events, muon events could be effectively extracted by excluding the ADC spectrum below ~200.

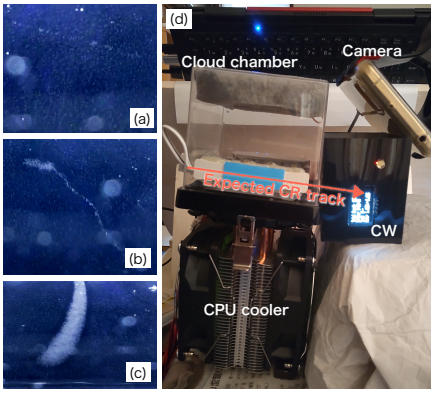

Figure 3: (a-c) Images of tracks in the cloud chamber. The tracks of (a), (b), and (c) correspond to a CR μ-, β-, and α-like event, respectively. (d) shows a setup of the bimodal experiment aiming at the coincident events between the chamber and the CW.

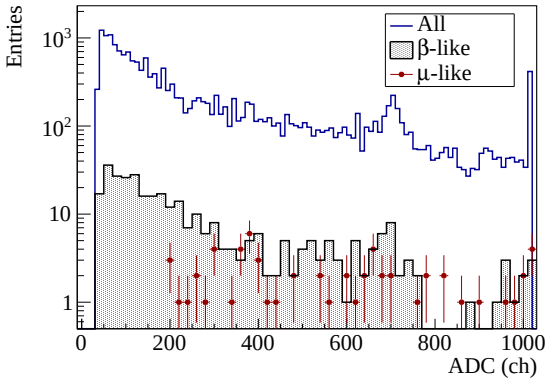

Figure 4: The obtained ADC spectra of the CW. The thin solid line shows the total event distribution. The hatched histogram is for β-like, and the filled circle with error bars is for μ-like events.

On the other hand, considering the geometrical configuration, the sampled events tend to hit in the center of the scintillator, and the resulting spectrum, especially of μ-like events, has such a bias. Thus the first conclusion above does not contradict the discussion in the previous section that muons penetrating the edge of the scintillator may yield a lower ADC values.

Improvements and developments are ongoing. For example, the current version of the cloud chamber has a small fiducial volume, which means that fewer events can be detected simultaneously with the CW, and only a small fraction of the events are available for particle identification. Therefore, we are developing another cloud chamber with a larger fiducial volume. To target cosmic ray muons, we should place the system at the zenith or closer. Also, the fact that we are using our eyes to identify particles poses problems in terms of quantity and efficiency. By improving the quality of the chamber, we expect an increase in the fraction of accurate trajectories captured. We also plan to use machine learning to identify images.

4. Case 3: Position resolution with stacked scintillators

Several applications require sensitivity to the arrival position of particles, such as muography, which estimates the internal density distribution of large structures from the direction and frequency

of muon arrival. The technique of reading out the SiPM from both ends of the scintillator array through layers of air, and to resolve the interaction position from the signal intensity ratio has been demonstrated by Kishimoto et al. [9] for inorganic scintillators and by Kuramoto et al. [10] for plastic scintillators. We expect a similar measurement to be possible using two pairs of CWs as readouts at both ends of plastic scintillators in a row. However, these previous studies aimed at gamma rays for the depth-of-interaction (DOI) resolution, so the number of events hitting multiple pixels is limited since multiple Compton scattering across pixels is relatively rare. When muons are the primary target of observation, as in this study, we expect that the number of events hitting multiple scintillators will increase. Therefore, the pattern of the signal ratio readout can be complex.

As shown in Figure 5, plastic scintillators for CW were stacked and assembled with a CW PCB with SiPMs at both ends. The scintillators form a one-dimensional array of three or five pieces jointed by an air layer. We then connected the analog signal output of the CW PCB to a single-board computer Red Pitaya STEMlab 125-10, and recorded the pulse heights from both ends for coincidence events. Students from Sendai Daisan High School performed runs with four configurations with the scintillator arrays aligned horizontally and vertically for the cases with 3-layer and 5-layer cases.

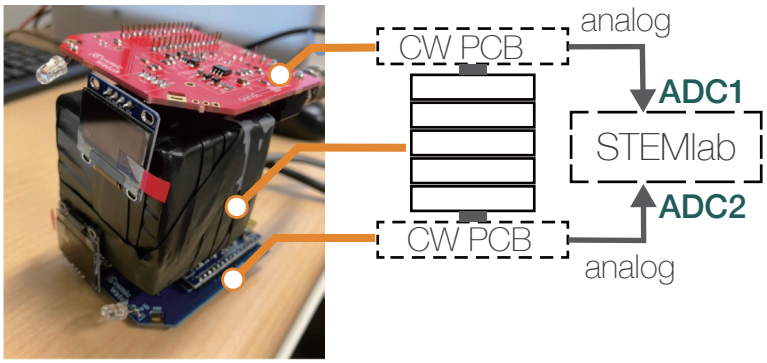

Figure 5: A photo of the fabricated detector system and a schematic of the components indicating the case with the 5 scintillators.

Figure 6 shows the correlation of the pulse heights of the signals from both ends in each measurement, from which much information could be extracted. In these figures, the events are distributed along the diagonal when the same number of photons reaches both ends. The central population in Figure 6(a) is considered to be near-vertical muon events that penetrated all three scintillators ("three-piece" events). Muons that penetrated one scintillators could produce two linear distributions with different slopes, and the two-piece events lie the intermediate curved regions. The total energy deposit is larger in the three-piece events, and the light yield should also be greater than in the one or two-piece events, as seen in the panel. Also, the distribution near zero could probably be the one-piece hit events with small energy deposit due to environmental background and random circuit noise.

Compared to the setup in Figure 6(a), in the case of (b) we expect an increase in the fraction of events where the vertically incident muon passes only one scintillator and a decrease in the number of three-piece events. The data obtained are consistent with the expectations, and the three linear

distributions should correspond to the one-piece muon events. Events with muons hitting multiple scintillators can be distributed between these straight lines. The crossing length becomes longer than in (a), and there is also an general trend towards larger energy deposits.

We expected a similar trend in the case of five scintillator layers. Figure 6(c) looks similar to (a) with an increase in total energy deposit due to the larger effective scintillator volume. Regarding (d), although the distribution was divided into several components, the five pieces could not be clearly separated. The diagonal component distribution appears slightly broader than in (b), probably contaminated by events hitting the inner scintillator blocks.

The main reason could be the lower efficiency in scintillation light transport due to the increased number of layers, which also leads to worse energy resolution. The overall distribution should result from the conflict between the increase in energy deposit and the decrease in light collection efficiency due to the increased number of layers. In (c), the volume increase was found to be more effective due to multi-piece events, while in (d), the transport loss was found to be more effective.

Further analysis is underway. The students are interested in particle identification from these combinations of ADC spectra. Investigating better position resolution may also be another research topic. Improving the light collection efficiency may be a critical issue.

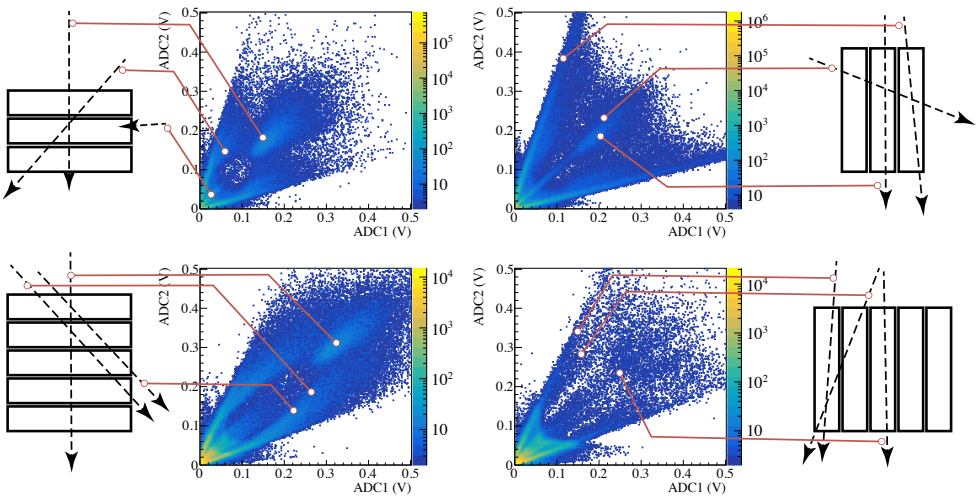

Figure 6: Correlation of pulse height of SiPMs for each end. Each panel corresponds to the 4 cases. (a) vertical array with 3 scintillators, (b) horizontal array with 3 scintillators, (c) vertical array with 5 scintillators, and (d) horizontal array with 5 scintillators. The arrangement of the detectors and possible ADC responses on the scatter plots are also illustrated.

5. Summary

CW is easy to use and is attractive as a student research instrument. The ADC spectrum obtained is considered to have the ability to separate muons from noise, albeit with limited accuracy; for CW alone, the spectrum should be cut at an ADC value of about 200 in a room temperature environment, and it would be even better if the cut value were temperature dependent. The results were supported by the spectral analysis and the cloud chamber experiments. The DOI detection capability can be

expected by the modifying the detector configuration, and it is expected to be used in the future as a way to utilize the CW PCB to reduce the installation cost of SiPM and readout circuit as the de facto standard.

Acknowledgement

This work was partially supported by Mitsubishi Memorial Foundation for Educational Excellence (Category 3).

References

[1] K. S. Tanaka et al., *Dialogue : Online Support for Cosmic-ray Research by Secondary Students at Tan-Q*, Japanese Journal of Science Communication 29, 37, 2021

[2] T. Nakamori, et al., *Collaboration between high schools in Japan and Argentina for cosmic-ray research using CosmicWatches*, PoS(ICRC 2021), 395, 1365, 2021

[3] H. Enomoto, et al., *Online support for research activities by high school and junior high school students*, PoS(ICRC 2023), 1600, 2023

[4] K. S. Tanaka, et al., *Radiation detectors fabricated by secondary students*, PoS(ICRC 2023), 1599, 2023

[5] S. N. Axani, K. Frankiesivcs, and J. M. Conrad, *The cosmicwatch desktop muon detector: self-contained, pocket sized particle detector*, Journal of Instrumentation, 13, P03918, 2018

[6] S. N. Axani, *The Physics Behind the CosmicWatch Desktop Muon Detectors*, arXiv:1908.00146, 2019

[7] K. Kumagai, et al., *Partial correlation between the frequency of muon detection on the ground in Akita Prefecture and the surface temperature, humidity, and atmospheric pressure for each weather*, J. of Science EGGS, 2110004, 1-6, 2021

[8] M. Akiyoshi, H. Ando, Y. Okuno, H. Matsuura, *Development of Radiological Educational Program Using a Peltier-Cooling-Type High Performance Cloud Chamber*, Proc. of ISRE2016, 54-62, 2017

[9] A. Kishimoto, et al., *Development of a dual-sided readout DOI-PET module using large-area monolithic MPPC-arrays*, IEEE-TNS, NS-60, 38, 2013

[10] M. Kuramoto, T. Nakamori, S. Kimura, S. Gunji, M, Takakura, J, Kataoka, *Development of TOF-PET using Compton scattering by plastic scintllators*, Nucl. Instr. Met. A, 845, 668-672, 2017